CHAPTER IV
RESULTS AND DISCUSSION

In this study, methane partial oxidation (MPO) to synthesis gas over Ceria-Nickel and Ceria-Zirconia-Nickel mixed oxides prepared via co-precipitation method that investigated over the temperature range of 400-800°C. The catalysts were calcined at either 500 or 700°C for 6 hr.

4.1 Catalyst Characterization

4.1.1 BET Surface Areas, Metal Dispersion

The BET surface areas and degrees of metal dispersion of the catalysts at different calcination temperatures are shown in Table 4.1. For a given catalyst calcined at 500°C and 700°C, the surface areas were found to decrease with increasing calcination temperature. When the calcination temperature was increased from 500 to 700°C, $(Ce_{0.75}Zr_{0.25})_{2.14}Ni_{0.86}O_3$ and $Ce_{2.14}Ni_{0.86}O_3$ surface areas were drastically decreased by about 30 and 18%, respectively. This might be due to the fact that nickel acts as a nucleating agent promoting the sintering and ceria, itself, has low thermal stability (Dong *et al.*, 2002). The drop in BET surface area may originate from the aggregation of mixed oxide phase, which indicates the structural properties significantly dependent on the calcination temperature. The degrees of metal dispersion determined by hydrogen chemisorptions were decreased as an increase in calcination temperature for both catalysts. However, the degree of metal dispersion of $Ce_{2.14}Ni_{0.86}O_3$ was lower than that of $(Ce_{0.75}Zr_{0.25})_{2.14}Ni_{0.86}O_3$. This might be due to the formation of NiO bulk particle encapsulation on $(Ce_{0.75}Zr_{0.25})_{2.14}Ni_{0.86}O_3$ catalyst.

Table 4.1 BET surface areas and degrees of metal dispersion of the catalysts at different calcination temperatures

Catalyst	Calcination temperature (°C)	BET surface area (m^2/g)	Metal dispersion (%)
$(Ce_{0.75}Zr_{0.25})_{2.14}Ni_{0.86}O_3$	500	53.3	5.8
	700	22.9	2.3
$Ce_{2.14}Ni_{0.86}O_3$	500	36.8	4.6
	700	8.2	1.7

4.1.2 Temperature-programmed Reduction by Hydrogen

The H_2-TPR profiles of the catalysts calcined at 500 and 700°C with a heating rate of 10°C min^{-1} are shown in Figure 4.1. For $(Ce_{0.75}Zr_{0.25})_{2.14}Ni_{0.86}O_3$ catalysts exhibits two kinds of peaks, one the maximum temperature at ca. 420°C is attributable to the reduction of bulk NiO, and the other peak maximum temperature at ca.600°C can be assigned to complex NiO_x species which strongly interaction with the support, and it seems to be concurrent with ceria reduction. The results are similar to that observed by Diskin *et al.* (1998) suggesting that low temperature peak are attributed to the reduction of NiO particles, while the higher temperature peak are attributed to the reduction of NiO in intimate contact with the oxide support which has stronger interaction with support. For $Ce_{2.14}Ni_{0.86}O_3$ catalysts, two obvious peaks appear the maximum temperature at ca. 380 and 500°C, respectively. It seems that

$Ce_{2.14}Ni_{0.86}O_3$ catalyst shifts downward, and thus overlaps the NiO reduction peak at about 500°C. It can be seen that $(Ce_{0.75}Zr_{0.25})_{2.14}Ni_{0.86}O_3$ catalysts are the most difficult to reduce which suggests that higher temperatures are needed in order to reduce the $(Ce_{0.75}Zr_{0.25})_{2.14}Ni_{0.86}O_3$ as compared to $Ce_{2.14}Ni_{0.86}O_3$. Moreover, this indicates a strong interaction between Ni and support, which helps produce mobile oxygen during the reaction.
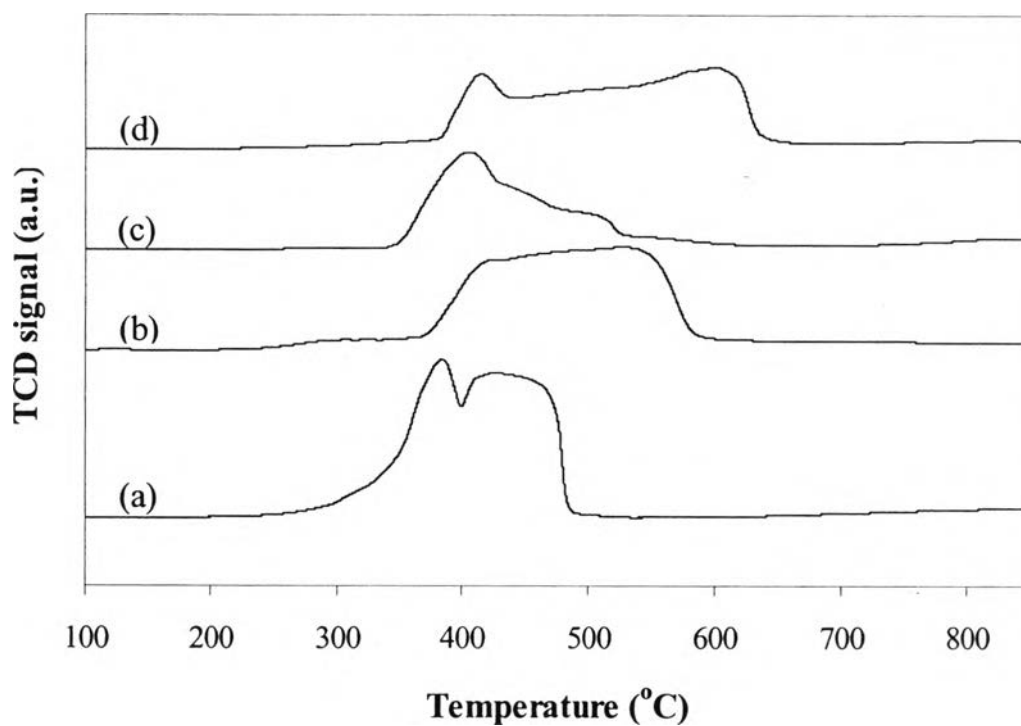

Figure 4.1 H_2-TPR profiles of the catalysts calcined at 500 and 700°C with a heating rate of 10°C min^{-1}: (a) $Ce_{2.14}Ni_{0.86}O_3$ (500°C), (b) $(Ce_{0.75}Zr_{0.25})_{2.14}Ni_{0.86}O_3$ (500°C), (c) $Ce_{2.14}Ni_{0.86}O_3$ (700°C), and (d) $(Ce_{0.75}Zr_{0.25})_{2.14}Ni_{0.86}O_3$ (700°C).

4.1.3 X-ray Diffraction

The XRD patterns of the samples calcined at different temperatures are shown in Figures 4.2. The results show that fresh $(Ce_{0.75}Zr_{0.25})_{2.14}Ni_{0.86}O_3$ and $Ce_{2.14}Ni_{0.86}O_3$ catalysts exhibited major peaks at about 29°, 33°, 48°, and 57° (2θ) indicating a cubic fluorite structure of CeO_2. Small peaks of NiO were observed at about 37°, 43°, and 63° (2θ). No separate phase due to Ni and NiO was detected. The results are similar to that $Ce_{0.75}Zr_{0.25}NiO_3$ and $CeNiO_3$ catalysts as can be seen in Figure 4.3. This might be attributed to NiO present in the form of nanoparticles (Pengpanich et al., 2008). Therefore, it was not possible to determine its crystallite size by XRD technique. The peak intensity was obviously strong with increasing calcination temperature. The results appeared similar with the BET surface area and metal dispersion data.
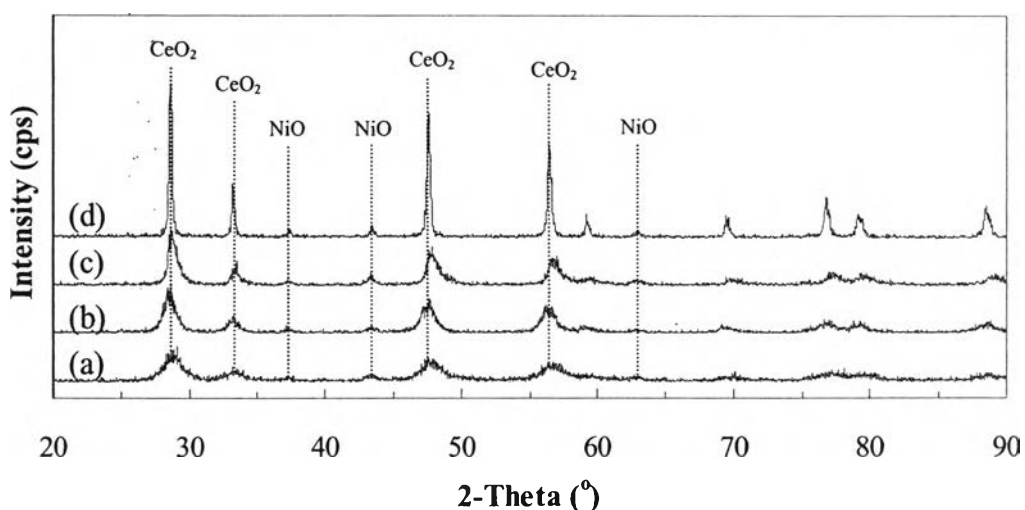

Figure 4.2 XRD patterns of $(Ce_{0.75}Zr_{0.25})_{2.14}Ni_{0.86}O_3$ and $Ce_{2.14}Ni_{0.86}O_3$ catalysts: (a) $(Ce_{0.75}Zr_{0.25})_{2.14}Ni_{0.86}O_3$ (500°C), (b) $Ce_{2.14}Ni_{0.86}O_3$ (500°C), (c) $(Ce_{0.75}Zr_{0.25})_{2.14}Ni_{0.86}O_3$ (700°C), and (d) $Ce_{2.14}Ni_{0.86}O_3$ (700°C), where the numerical values in parentheses represent the calcination temperatures.
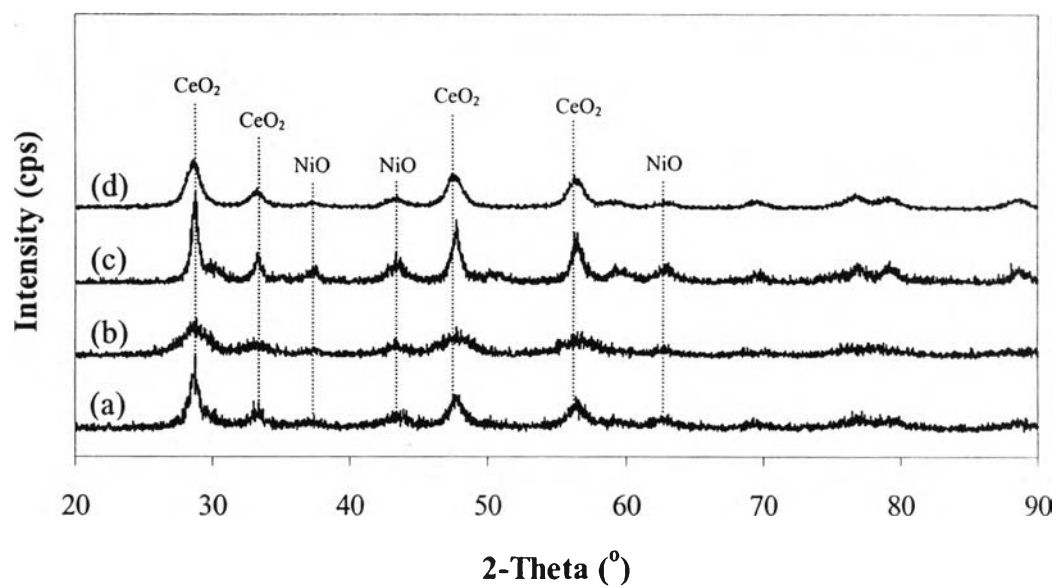
Figure 4.3 XRD patterns of $Ce_{0.75}Zr_{0.25}NiO_3$ and $CeNiO_3$ catalysts: (a) $Ce_{0.75}Zr_{0.25}NiO_3$ (500°C), (b) $CeNiO_3$ (500°C), (c) $Ce_{0.75}Zr_{0.25}NiO_3$ (700°C), and (d) $CeNiO_3$ (700°C).

4.2 Catalytic Activity Tests for Methane Partial Oxidation

4.2.1 Catalytic Activity Tests

The catalytic activity of the catalysts for MPO to synthesis gas was tested in a dilute mixture (4% CH_4 and 2% O_2 balanced with He) in the temperature range of 400–800°C. The CH_4 conversion, H_2 and CO selectivity as a function of temperature for MPO are shown in Figures 4.4 and 4.5. The synthesis gas products (CO and H_2) and CH_4 conversion with the complete oxidation products of $(Ce_{0.75}Zr_{0.25})_{2.14}Ni_{0.86}O_3$ and $Ce_{2.14}Ni_{0.86}O_3$ were observed at temperatures higher than that of $Ce_{0.75}Zr_{0.25}NiO_3$ and $CeNiO_3$. Under such conditions, the light hydrocarbons produced by cracking reactions were then further reformed by either CO_2 or H_2O to yield CO and H_2 products (Pena $et\ al.$, 1996). Beyond a temperature of 600°C the methane conversion dramatically increases resulting from the methane partial oxidation reaction. The results are similar to that observed by Shishido $et\ al.$ (2002) suggesting that the first stage was corresponding to the combustion of methane followed by steam and CO_2 reforming reactions of methane to synthesis gas. The CH_4 conversion, CO selectivity and H_2 selectivity at 750°C are about 97%, 93% and 90%, respectively, for the $(Ce_{0.75}Zr_{0.25})_{2.14}Ni_{0.86}O_3$ catalyst calcined at 500°C. In comparison, about 94% CH_4 conversion, 92% CO selectivity and 88% H_2 selectivity were achieved for the $Ce_{2.14}Ni_{0.86}O_3$ catalyst calcined at 500°C. The results are similar to that the $Ce_{0.75}Zr_{0.25}NiO_3$ catalyst calcined at 500°C. This suggests that $(Ce_{0.75}Zr_{0.25})_{2.14}Ni_{0.86}O_3$ and $Ce_{0.75}Zr_{0.25}NiO_3$ catalysts calcined at 500°C give higher MPO catalytic activity and selectivity to synthesis gas than $Ce_{2.14}Ni_{0.86}O_3$ and $CeNiO_3$ catalysts calcined at 500°C. With increasing calcination temperature, CH_4 conversion for $(Ce_{0.75}Zr_{0.25})_{2.14}Ni_{0.86}O_3$ and $Ce_{0.75}Zr_{0.25}NiO_3$ catalysts were insignificantly decreased (ca. 3%) due to the decrease in surface area. However, CO and H_2 selectivities were slightly increased. This might be due to that it is favorable to produce more oxygen vacancies in which active oxygen species are formed (Xiaoping $et\ al.$, 2008).
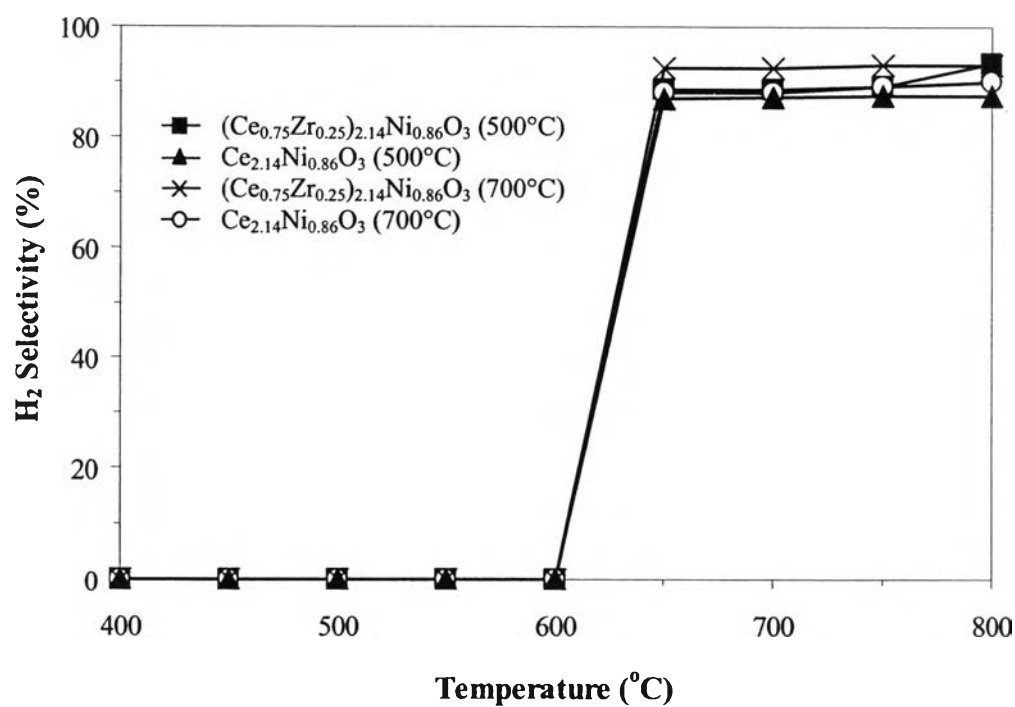
(a)
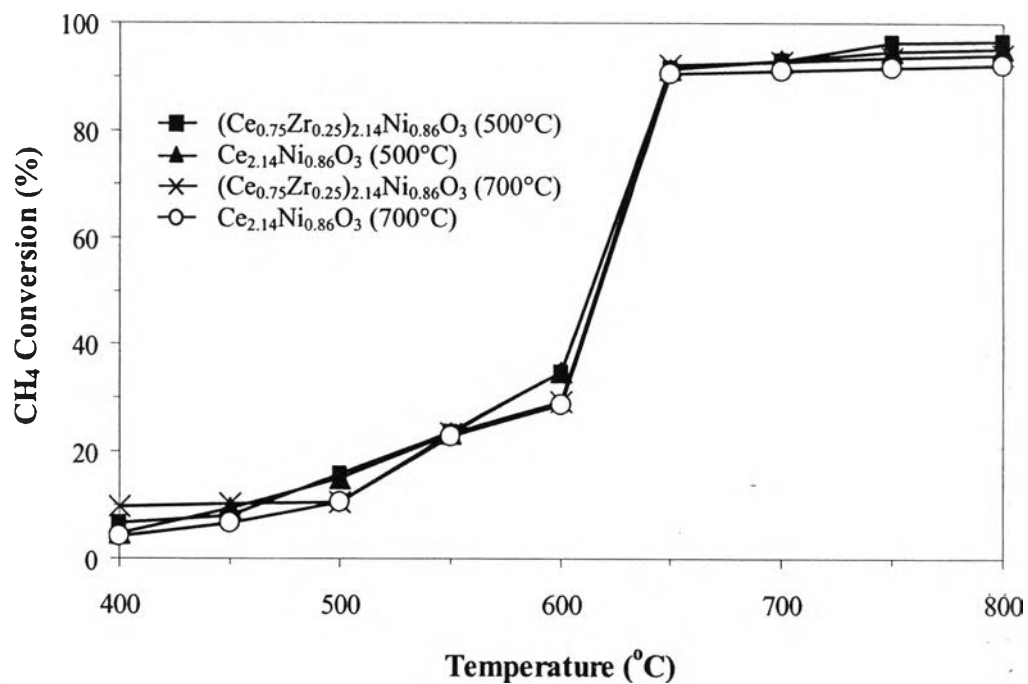
(b)

Figure 4.4 The CH_4 conversion (a), H_2 selectivity (b), and CO selectivity (c) of $(Ce_{0.75}Zr_{0.25})_{2.14}Ni_{0.86}O_3$ and $Ce_{2.14}Ni_{0.86}O_3$ for methane partial oxidation.
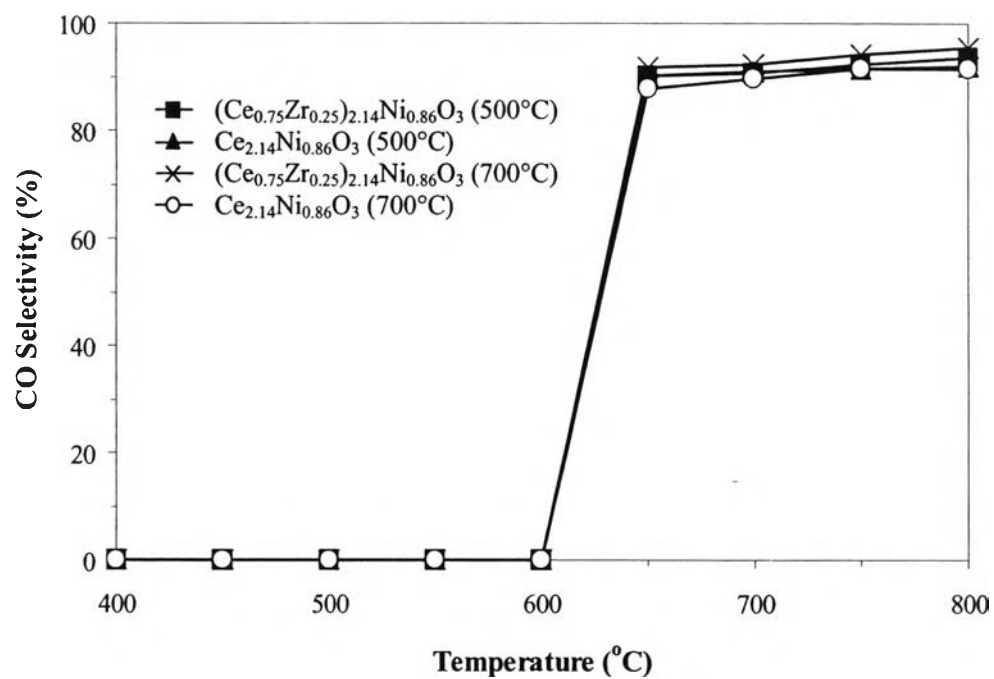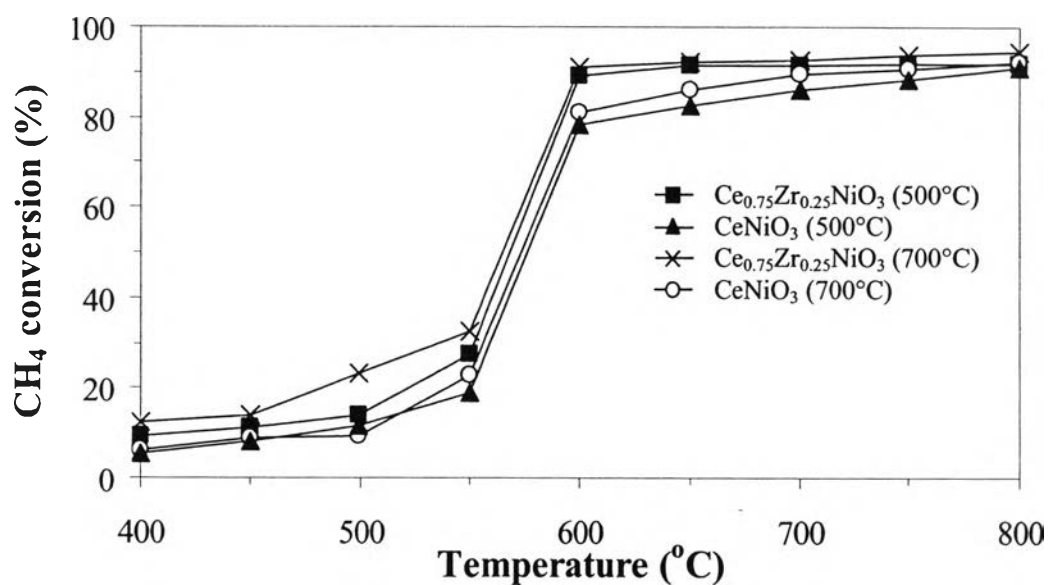
(c)

Figure 4.4 (cont.) The CH_4 conversion (a), H_2 selectivity (b) and CO selectivity (c) of $(Ce_{0.75}Zr_{0.25})_{2.14}Ni_{0.86}O_3$ and $Ce_{2.14}Ni_{0.86}O_3$ for methane partial oxidation.
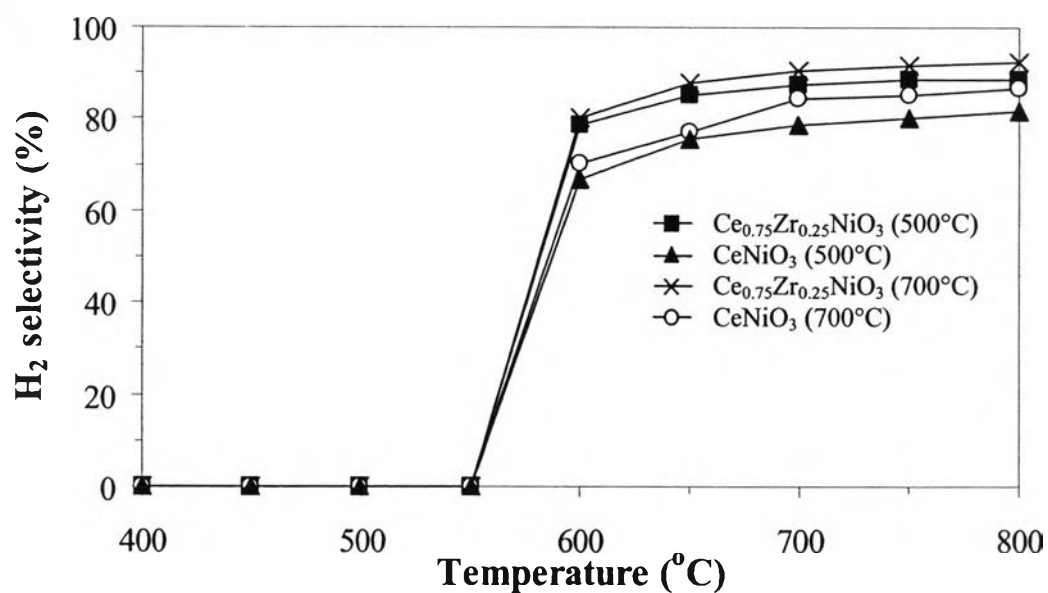
(a)

(b)

Figure 4.5 The CH_4 conversion (a), H_2 selectivity (b) and CO selectivity (c) of $Ce_{0.75}Zr_{0.25}NiO_3$ and $CeNiO_3$ for methane partial oxidation.

(c)

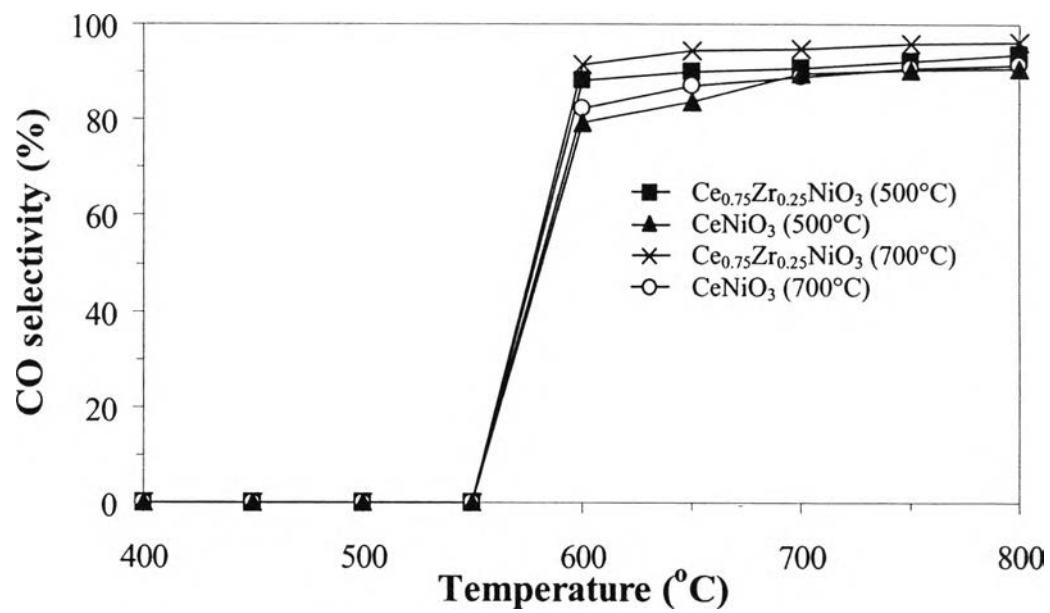**Figure 4.5 (cont.)** The CH_4 conversion (a), H_2 selectivity (b) and CO selectivity (c) of $Ce_{0.75}Zr_{0.25}NiO_3$ and $CeNiO_3$ for methane partial oxidation.

4.2.2 Carbon Deposition

As seen in Figures 4.6 and 4.7, at 750°C, the methane conversion, H_2 and CO selectivity as a function of time on stream of catalysts remained unchanged under MPO. This suggested that the catalysts stable in the presence of stream. Since carbon deposition was not observed for the spent catalysts at 750°C after 24 hr on stream.

The amount of carbon deposition on the catalysts after running the reaction for 24 hr of reaction at 750°C and CH_4/O_2 ratio of 2 is shown in Table 4.2. The amount of carbon deposition on the spent catalysts was quantified by TPO technique, the amount of carbon deposition was found rarely decrease with the calcinations temperature increased. This indicated that the carbon deposition is strongly inhibited when the calcination temperature increased. It seems to be that the amount of carbon deposition on $(Ce_{0.75}Zr_{0.25})_{2.14}Ni_{0.86}O_3$ was lower than that of $Ce_{2.14}Ni_{0.86}O_3$. This might be due to the fact that higher reducibility than $Ce_{2.14}Ni_{0.86}O_3$ confirmed by TPR results.

As can be seen in Figure 4.8, the TPO profiles of catalysts show peak centered at ca. 350 and 500°C, except for $Ce_{2.14}Ni_{0.86}O_3$ calcined at 500°C show an additional peak centered at temperature of ca. 630°C. The results are similar to that observed by Pengpanich et al. (2004) suggesting that the peaks observed on the TPO profiles can be due to the presence of different types of carbon or different sites of carbon deposition. Moreover, Koerts et al. (1991) have identified three types of surface carbonaceous species generated by methane decomposition: C^α (or carbidic carbon can be hydrogenated at temperatures below 50°C), C^γ (or amorphous carbon, hydrogenable between 100 and 300°C), and C^β (or graphitic carbon, hydrogenable at temperatures > 400°C). The carbon depositions on the spent catalysts are confirmed by TEM images as shown in Figure 4.9. Both of the spent $(Ce_{0.75}Zr_{0.25})_{2.14}Ni_{0.86}O_3$ and $Ce_{2.14}Ni_{0.86}O_3$ catalysts calcined at 700°C, the types of carbon deposition appeared amorphous rather than whisker form as compared with $Ni/Ce_{0.75}Zr_{0.25}O_2$ as shown in Figure 4.10.
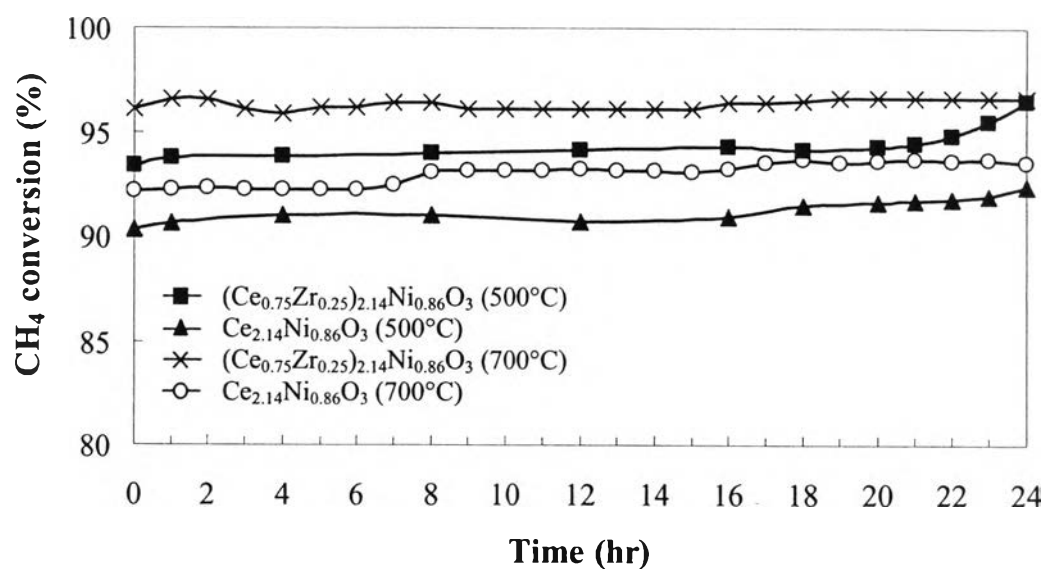
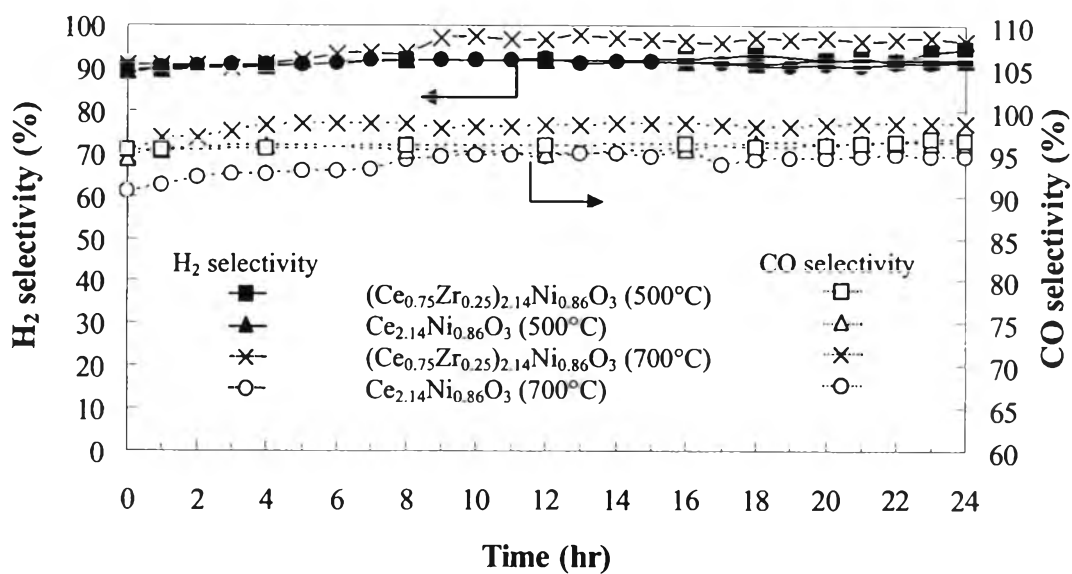**Figure 4.6** The CH_4 conversion as a function of time at 750°C.

Figure 4.7 H_2 and CO selectivities as a function of time at 750°C.

Table 4.2 The amount of carbon deposition quantified by TPO over the catalysts after 24 hr of reaction at 750°C and CH_4/O_2 ratio of 2

Catalyst	Calcination temperature (°C)	X_{CH_4}[a] (%)	S_{CO}[a] (%)	S_{H_2}[a] (%)	Amount of carbon (wt.%)
$(Ce_{0.75}Zr_{0.25})_{2.14}Ni_{0.86}O_3$[b]	500	97	96	94	0.85
	700	96	98	96	0.62
$Ce_{2.14}Ni_{0.86}O_3$[b]	500	93	95	91	1.41
	700	92	95	92	1.12

[a] measured at the end of reaction time
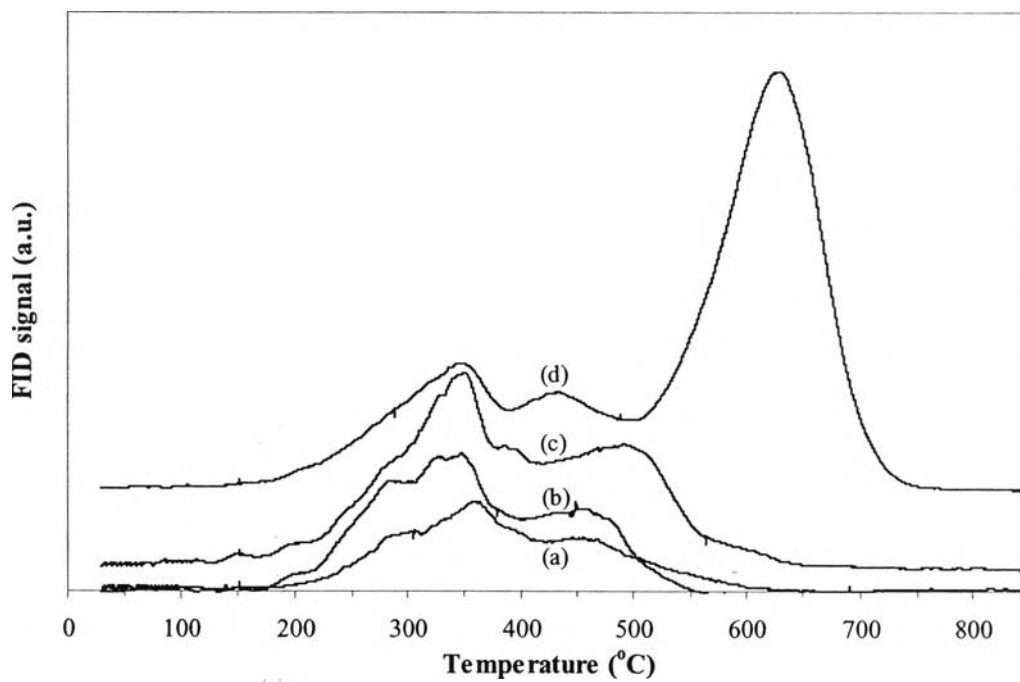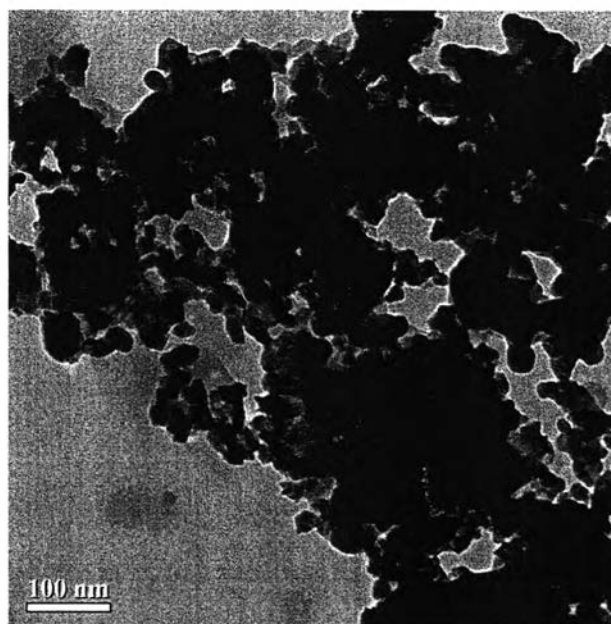
[b] after 24 hr reaction at 750°C and CH_4/O_2 ratio of 2.0

Figure 4.8 TPO profiles of catalysts after exposure to reaction at 750°C for 24 hr:
(a) $(Ce_{0.75}Zr_{0.25})_{2.14}Ni_{0.86}O_3$ (700°C), (b) $(Ce_{0.75}Zr_{0.25})_{2.14}Ni_{0.86}O_3$ (500°C), (c) $Ce_{2.14}Ni_{0.86}O_3$ (700°C), (d) $Ce_{2.14}Ni_{0.86}O_3$ (500°C).

(a)

(b)

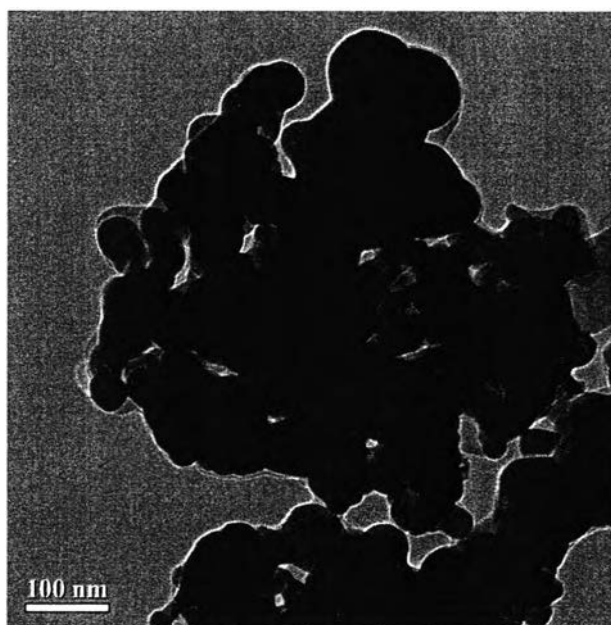**Figure 4.9** TEM images of spent catalysts calcined at 700°C: (a) $(Ce_{0.75}Zr_{0.25})_{2.14}Ni_{0.86}O_3$, (b) $Ce_{2.14}Ni_{0.86}O_3$, where measure after exposure reaction at 750°C for 24 hr.
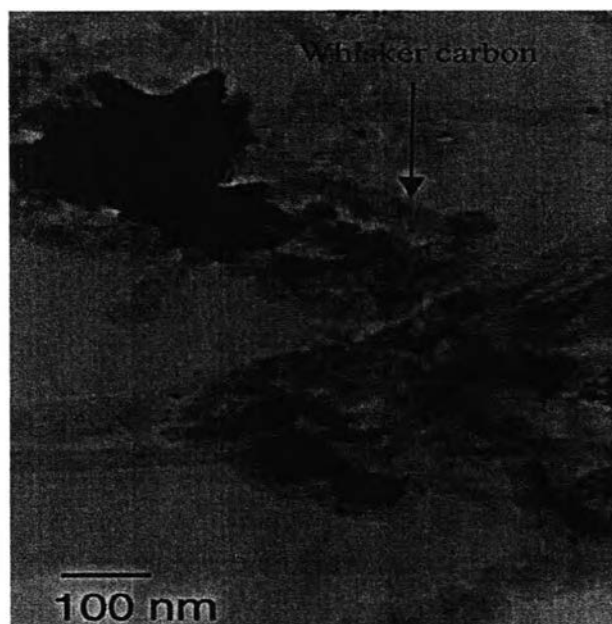
Figure 4.10 TEM images of Ni/Ce$_{0.75}$Zr$_{0.25}$O$_2$ after exposure reaction at 750°C for 24 hr.